

## Standard neutrino spectrum from ${}^8\text{B}$ decay

John N. Bahcall and E. Lisi\*

*Institute for Advanced Study, Princeton, New Jersey 08540*

D. E. Alburger

*Brookhaven National Laboratory, Upton, New York 11973*

L. De Braekeleer

*Department of Physics, University of Washington, Seattle, Washington 98195*

S. J. Freedman

*Department of Physics and Lawrence Berkeley National Laboratory, University of California, Berkeley, California 94720*

J. Napolitano

*Rensselaer Polytechnic Institute, Troy, New York 12180*

(Received 14 November 1995; revised manuscript received 18 March 1996)

We present a systematic evaluation of the shape of the neutrino energy spectrum produced by beta decay of  ${}^8\text{B}$ . We place special emphasis on determining the range of uncertainties permitted by existing laboratory data and theoretical ingredients (such as forbidden and radiative corrections). We review and compare the available experimental data on the  ${}^8\text{B}(\beta^+){}^8\text{Be}(2\alpha)$  decay chain. We analyze the theoretical and experimental uncertainties quantitatively. We give a numerical representation of the best-fit (standard-model) neutrino spectrum, as well as two extreme deviations from the standard spectrum that represent the total (experimental and theoretical) effective  $\pm 3\sigma$  deviations. Solar neutrino experiments that are currently being developed will be able to measure the shape of the  ${}^8\text{B}$  neutrino spectrum above about 5 MeV. An observed distortion of the  ${}^8\text{B}$  solar neutrino spectrum outside the range given in the present work could be considered as evidence, at an effective significance level greater than three standard deviations, for physics beyond the standard electroweak model. We use the most recent available experimental data on the Gamow-Teller strengths in the  $A = 37$  system to calculate the  ${}^8\text{B}$  neutrino absorption cross section on chlorine:  $\sigma_{\text{Cl}} = (1.14 \pm 0.11) \times 10^{-42} \text{ cm}^2$  ( $\pm 3\sigma$  errors). The chlorine cross section is also given as a function of the neutrino energy. The  ${}^8\text{B}$  neutrino absorption cross section in gallium is  $\sigma_{\text{Ga}} = (2.46^{+2.1}_{-1.1}) \times 10^{-42} \text{ cm}^2$  ( $\pm 3\sigma$  errors). [S0556-2813(96)01307-6]

PACS number(s): 96.60.Jw, 23.40.Bw, 26.65.+t, 27.20.+n

### I. INTRODUCTION

The solar neutrino spectrum is currently being explored by four underground experiments: the pioneering Homestake (chlorine) detector [1], the Kamiokande (water-Cherenkov) detector [2], and two gallium detectors GALLEX [3] and SAGE [4].

These first-generation experiments have shown that the observed solar neutrino event rates are lower than expected [5], giving rise to “solar neutrino problems” [6] that cannot be solved within the standard experimental and theoretical understanding of the physics of the Sun and of the electroweak interactions.

Bahcall [7] has shown that the  ${}^8\text{B}(\beta^+){}^8\text{Be}$  (allowed) decay produces the same shape for the ( ${}^8\text{B}$ ) neutrino spectrum, up to gravitational redshift corrections of  $O(10^{-5})$ , independent of whether the neutrinos are created in a terrestrial laboratory or in the center of the Sun. Thus, experimental evidence for a deviation of the  ${}^8\text{B}$  solar neutrino spectrum from the laboratory shape would constitute evidence for physics

beyond the standard model of the electroweak interactions. Indeed, powerful new experiments, such as the SuperKamiokande [8], the SNO [9], and the ICARUS [10] detectors, will measure the *shape* of the high-energy ( $E_\nu \gtrsim 5$  MeV) part of the solar neutrino spectrum, which originates from the beta decay of  ${}^8\text{B}$  produced in the Sun.

The calculation of the  ${}^8\text{B}$  solar neutrino spectrum dates back to 1964, when it was pointed out [11] that the usual  $\beta$ -decay allowed spectrum should be averaged over the intermediate  $2^+$  states of  ${}^8\text{Be}$ , as derived by the subsequent alpha decay  ${}^8\text{Be}(2\alpha)$ . Experimental evidence for this smearing was found 23 years later in the associated positron spectrum [12]. The calculation of the spectrum has been continually improved by Bahcall and collaborators in [11,13,14], to which we refer the conscientious reader for all the details not reported here. The independent calculation of the  ${}^8\text{B}$  neutrino spectrum by Napolitano *et al.* [12] also compares well with the results in [14].

In this work, the evaluation of the  ${}^8\text{B}$  solar neutrino spectrum is further improved, using recently available experimental data and new theoretical calculations. Moreover, the maximum uncertainties ( $\pm 3$  effective standard deviations) that can affect the best estimated spectrum are determined. The inferred spectral shape is presented numerically and

\*Also at Dipartimento di Fisica and Sezione INFN di Bari, Bari, Italy.

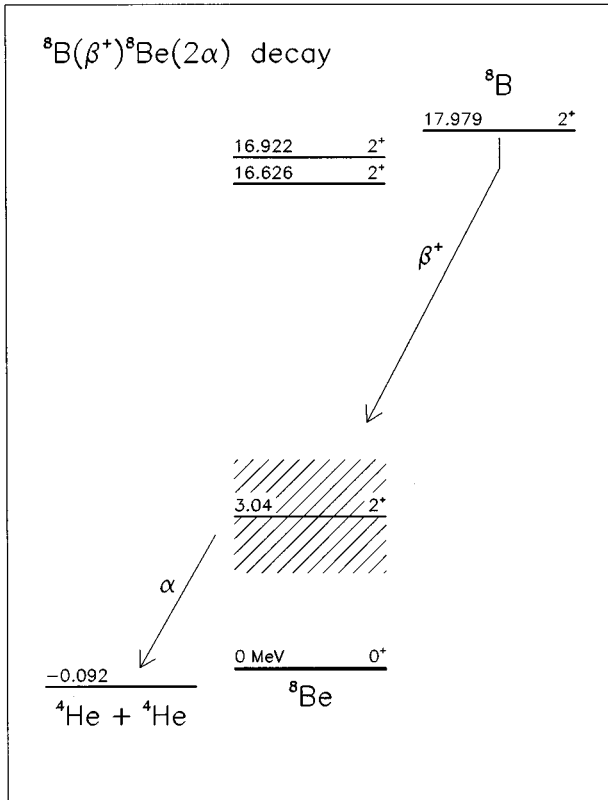


FIG. 1. Energy levels in the  ${}^8\text{B}(\beta^+){}^8\text{Be}(2\alpha)$  decay chain (not to scale).

graphically, in forms useful for fits to experimental results and for phenomenological analyses. The neutrino spectra, together with new data on the Gamow-Teller strengths in the  $A=37$  system, are used to improve the calculations of the  ${}^8\text{B}$  neutrino absorption cross sections for chlorine and for gallium.

The paper is organized as follows. In Sec. II, the available experimental data on the  ${}^8\text{B}(\beta^+){}^8\text{Be}(2\alpha)$  decay chain are reviewed and discussed, in order to extract an optimal data set and in order to evaluate the experimental uncertainties. In Sec. III the best neutrino spectrum is calculated, including the appropriate radiative corrections. The total (theoretical and experimental) uncertainties are used to calculate a “ $+3\sigma$ ” and a “ $-3\sigma$ ” spectrum, characterizing the maximum deviations from the optimal spectrum. In Sec. IV these spectra are applied to a refined calculation of the  ${}^8\text{B}$  neutrino absorption cross sections for  ${}^{37}\text{Cl}$  and for  ${}^{71}\text{Ga}$ . A summary of the work is presented in Sec. V.

## II. EXPERIMENTAL DATA ON THE ${}^8\text{B}(\beta^+){}^8\text{Be}(2\alpha)$ DECAY CHAIN

In this section, we present a compilation of the available experimental data on beta and alpha decay of  ${}^8\text{B}$ . Then the various  $\alpha$ -decay data are compared and used to fit the  $\beta$ -decay data. The best-fit alpha spectrum and its  $\pm 3\sigma$  range emerge naturally from this overconstrained comparison.

The  $\beta$  decay of  ${}^8\text{B}$  populates  $2^+$  states in  ${}^8\text{Be}$ , which then breaks up into two  $\alpha$  particles [15]. The energy levels are shown in Fig. 1. The  $\beta$ ,  $\alpha$ , and correlated  $\beta$ - $\alpha$  spectra have been investigated by several experimental groups. In

addition to the solar neutrino application, this decay chain is of special interest because the  $A=8$  nuclear isotriplet (Li, Be, B) can be used to search for violations of the conserved vector current (CVC) hypothesis or for the existence of second-class currents (SCC’s) (see, e.g., the review [16]), and is also an interesting subject for  $R$ -matrix analyses [17–19].

For the determination of the  ${}^8\text{B}$  (solar) neutrino spectrum, a single precise determination of the alpha spectrum is, in principle, all that is required. In practice, we take advantage of the redundancy of the available experimental information to estimate both a preferred alpha spectrum and the possible uncertainties.

### A. Beta-decay data

The most recent determination of  ${}^8\text{B}$   $\beta$ -decay spectrum is reported (graphically) in [12]. The original number of detected counts in each of the 33 channels used (for momentum  $p \geq 9$  MeV) has been made available by one of us (J.N.). We discuss below in detail the energy calibration of the  $\beta$ -decay data of [12], for its particular relevance to the present work.

The calibration procedure used in [12] was similar to that in [20], which employed the same spectrograph to determine the weak magnetism correction to the  ${}^{12}\text{B}$   $\beta$ -spectrum shape. In [12], the  ${}^{12}\text{B}$  spectrum itself was used to set the calibration. The  ${}^{12}\text{B}$  source was produced through the  ${}^{11}\text{B}(d,p)$  reaction, with the spectrograph fixed at the same field setting used for the  ${}^8\text{B}$  data. The momentum measurement was in channels corresponding to a position along the focal plane. Prior studies of the spectrograph [21] demonstrated good linearity between momentum and position. The  ${}^{12}\text{B}$  raw data ( $\sim 1.1 \times 10^5$  counts) were collected in 36 momentum bins. The data were fitted with the standard allowed  $\beta$ -decay spectrum, along with the known recoil order corrections (see [20] and references therein). Both the normalization and the offset in the position relative to the radius of curvature were left free in the fit. The simultaneous minimization of  $\chi^2$  with respect to these two parameters yielded a good fit ( $\chi^2/N_{\text{DF}}=1.1$ ), and showed no evidence for a systematic deviation in the residuals. The error in the absolute momentum calibration was estimated to be less than 0.2% at  $1\sigma$ . Our conservative estimate for the maximum ( $\pm 3\sigma$ ) uncertainty in the energy calibration of the  $\beta$ -decay data in [12] is  $\delta E_\beta = \pm 0.090$  MeV. This value corresponds to 3 times a  $\pm 0.2\%$  error at the end-point energy  $E_\beta \approx 15$  MeV.

As we will see, the  $\beta$ -decay spectrum data of [12] play a fundamental role in constraining the uncertainties of the neutrino energy spectrum. Attempts to confirm the positron spectrum data, including measurements at lower momenta, would be helpful. Unfortunately, existing additional data on the  ${}^8\text{B}$   $\beta$ -decay as reported (only graphically) in  $\beta$ - $\alpha$  correlation searches [22,23] are too sparse to be useful for our purposes.

### B. Alpha decay data

Figure 2 shows our compilation of the experimental data for the delayed  $\alpha$  spectrum. The measurements with the highest statistics have been performed by Wilkinson and Alburger [24], using both a thick and a thin catcher (WA1 and

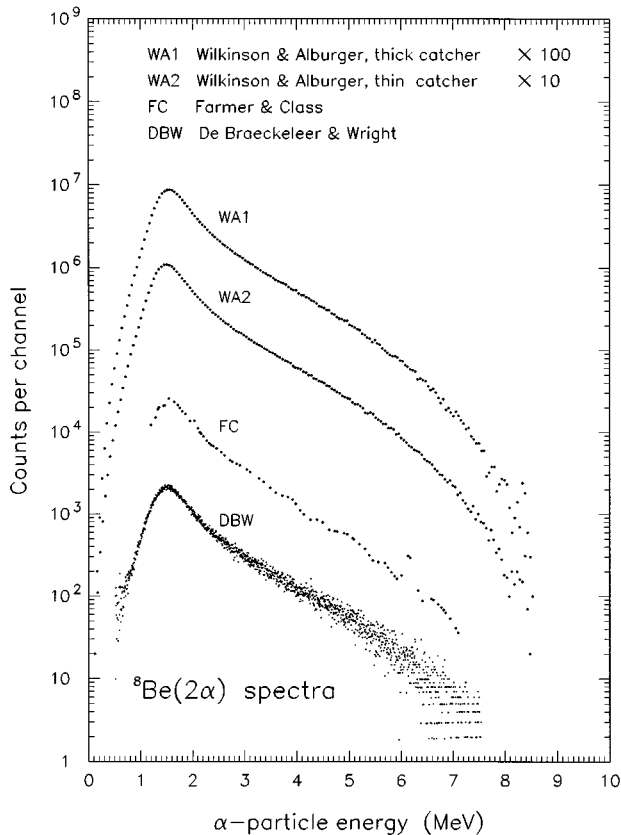


FIG. 2. Compilation of  ${}^8\text{Be}(2\alpha)$  decay data. The bin widths are different for different experiments. The data WA1 and WA2 are shifted on the vertical axis.

WA2 in Fig. 2, respectively). For our purposes, it is sufficient to know that the typical energy loss of  $\alpha$  particles is  $\sim 100$  ( $\sim 50$ ) keV in the thick (thin) catcher. The WA1 data ( $\sim 2.1 \times 10^6$  counts) have been reported by Warburton [18], together with the proper channel-energy calibration formula. Barker [19] has described similarly the WA2 data ( $\sim 2.5 \times 10^6$  counts). An older measurement of the  $\alpha$  spectrum was performed by Farmer and Class [25], although reported only in a graphical form (Fig. 2 in [25]). The spectrum labeled “FC” in Fig. 2 corresponds to a digitized form of their data ( $\sim 0.5 \times 10^6$  counts). A high-statistics data set has been also collected by one of us (L.DeB.) and D. Wright, in the course of a recent experimental search for CVC violation and SCC effects in the  $A = 8$  multiplet [26]. These data ( $\sim 1.6 \times 10^6$  counts) are labeled as “DBW” in Fig. 2.

In all of the  $\alpha$ -decay measurements we use, the experimentalists devoted considerable attention to the  $\alpha$  energy calibration, and in particular to the accurate estimate of the energy loss in the target. The spectra were corrected by the experimentalists for calibration and energy loss effects. We do not use the  $\alpha$  spectrum measured by Clark *et al.* in [27], since data cannot be extracted from their Fig. 2 with sufficient precision to be useful for our purposes.

The spectra in Fig. 2 are peaked at  $E_{\text{peak}} \approx 1.5$  MeV and decrease very rapidly for  $E_{\alpha} \neq E_{\text{peak}}$  (notice the logarithmic scale). At  $1.5_{-0.7}^{+1.8}$  MeV, the spectral values are decreased by a factor  $\sim 10$ . The interval  $1.5_{-0.7}^{+1.8}$  MeV contains  $\sim 90\%$  of the experimental counts for each data set. Therefore the

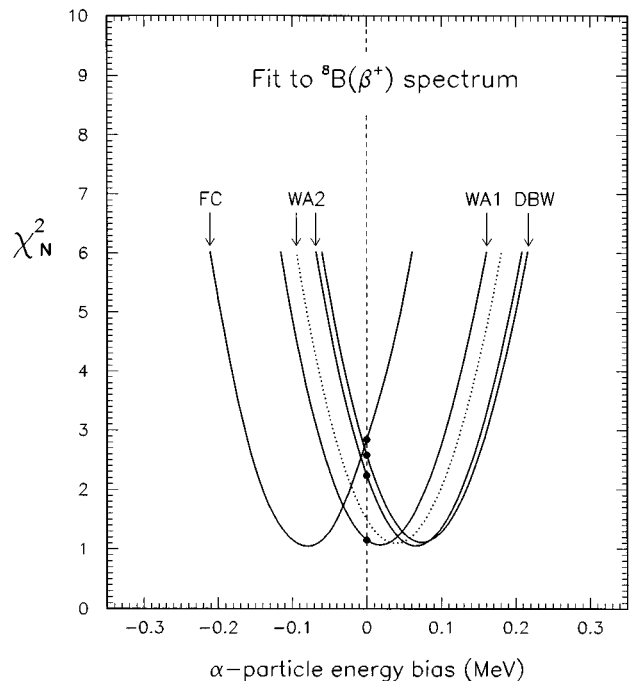


FIG. 3. Values of the normalized chi square in a fit to the experimental positron spectrum, using the input alpha decay data of Fig. 2, with an allowance for a possible bias,  $b$ , in the detected  $\alpha$  particle energy. The curves are remarkably similar, modulo a constant bias.

“tails” of the spectra ( $E_{\alpha} \leq 0.8$  MeV and  $E_{\alpha} \geq 3.3$  MeV) contribute only  $\sim 10\%$  to the smearing of the end-point energies in the calculation of the neutrino or positron spectra from  ${}^8\text{B}$  decay.

### C. Discussion of experimental uncertainties

A close inspection of Fig. 2 reveals that the four different  $\alpha$ -decay spectra WA1, WA2, FC, and DBW have slightly displaced peaks, with a total spread in the peak energies of about  $\pm 0.08$  MeV. Indeed, the largest uncertainty in these spectra can be ascribed to a possible bias  $b$  in the measured alpha particle energy:  $E_{\alpha} \rightarrow E_{\alpha} + b$ . If the intermediate  $2^+$  state at 3.04 MeV (see Fig. 1) were a narrow resonance, then  $b$  could be taken as a constant bias. In general,  $b$  may depend on  $E_{\alpha}$ , since in fact the intermediate state is not very narrow; thus the bias might assume slightly different values at the peak or in the tails of the  $\alpha$ -decay spectra. However, in the calculation of the  ${}^8\text{B}$  neutrino spectrum the  $\alpha$ -spectrum tails are much less important than the peak region ( $0.8 \leq E_{\alpha} \leq 3.3$  MeV), so that  $b$  is assumed to be a constant ( $b = b_{\text{peak}}$ ) for our purposes.

For the spectra WA1 and WA2, Barker has given in [19] a thorough discussion and an estimate of the possible contributions to  $b$ , including uncertainties due to energy loss, calibration, and finite resolution. A succinct summary of Barker’s analysis is that  $|b| \leq 0.05$  MeV at  $1\sigma$ . In particular, for the spectrum WA2 (thin catcher), two possible channel-energy calibration formulas are presented in [19] [see Eqs. (1) and (15) therein], which differ by  $\sim 0.05$  MeV in the alpha-energy peak. The first calibration [Eq. (1) in Barker’s paper] has been used in connection with the spectrum WA2 shown

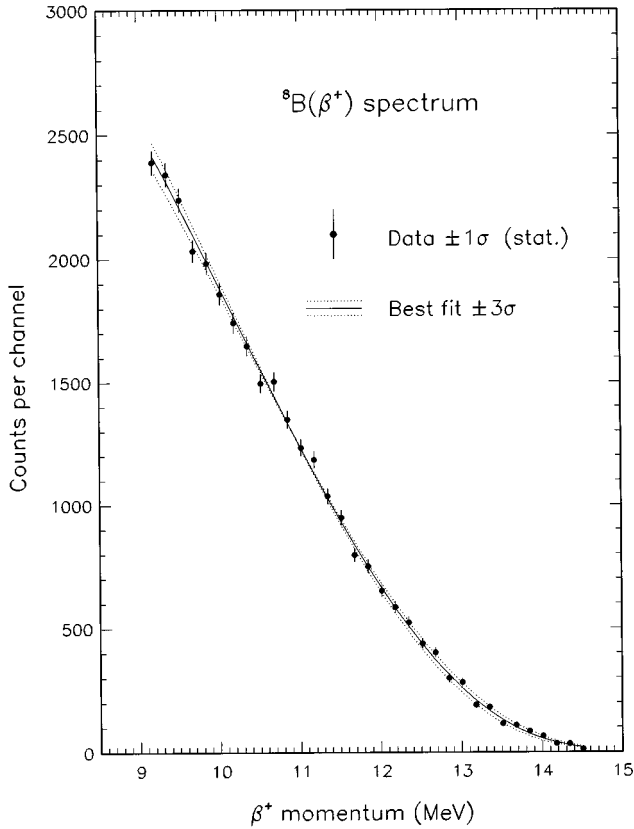


FIG. 4. Experimental data on the positron spectrum, together with the best fit and the  $\pm 3\sigma$  fits, corresponding to WA1 alpha decay data within the bias range  $b = 0.025 \pm 0.056$  MeV.

in Fig. 2; the second calibration will be used below for a further check of the sensitivity of the inferred spectrum to possible systematic uncertainties. For the DBW spectrum, the uncertainty in  $E_\alpha$  is estimated to be of comparable magnitude ( $\sim 0.04$  MeV) [26]. The uncertainty is larger ( $|b| \leq 0.1$  MeV) for the older FC spectrum [25], in part as a result of the necessity of converting to graphical data.

Each of the four  $\alpha$  particle data sets can be used to estimate the theoretical positron spectrum in  ${}^8\text{B}(\beta^+){}^8\text{Be}$  decay. The ingredients of this calculation are the same as for the neutrino spectrum, except for the radiative corrections. In fact, in beta decay the radiative corrections take a different form according to whether the  $\beta$  particle or the neutrino is detected. In the first case, they have been computed by Sirlin [28]. In the second case, they have been recently evaluated by Batkin and Sundaresan [29], and will be discussed later (in Sec. III). The computed positron spectrum, including radiative corrections, is then compared to the experimental  $\beta$ -decay data (33 points) as in [12]. The total number of counts collected ( $\sim 0.3 \times 10^6$ ) is used for normalization, reducing the number of degrees of freedom ( $N_{\text{DF}}$ ) to 32. A normalized  $\chi^2_N$  ( $\chi^2_N = \chi^2/N_{\text{DF}}$ ) is then calculated for each input  $\alpha$  spectrum, and this exercise is repeated also by shifting the experimental  $\alpha$  energy values ( $E_\alpha \rightarrow E_\alpha + b$ ). In the calculation of  $\chi^2_N$  we include the statistical errors of the  $\beta$ -decay data but exclude, in first approximation, their energy calibration uncertainty  $\delta E_\beta$  (Sec. II A). The effect of this additional uncertainty is discussed at the end of this section.

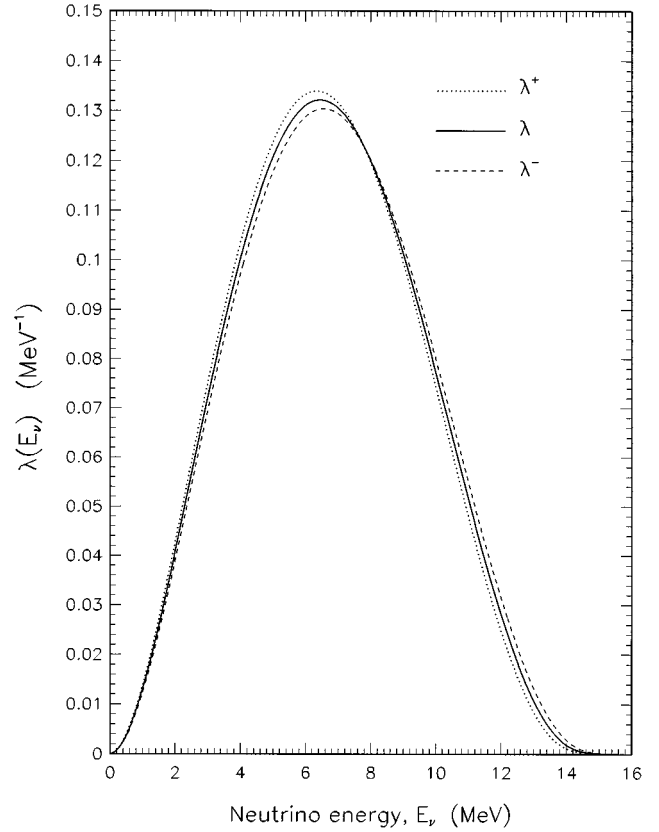


FIG. 5. The best-estimate (standard)  ${}^8\text{B}$  neutrino spectrum  $\lambda$ , together with the spectra  $\lambda^\pm$  allowed by the maximum ( $\pm 3\sigma$ ) theoretical and experimental uncertainties.

Figure 3 shows, for each of the four measured  $\alpha$  particle spectra, the normalized  $\chi^2$  fit to the measured positron spectrum as a function of the assumed  $\alpha$  particle energy bias. For zero energy bias (vertical dashed line) the FC, DBW, WA2, and WA1 data provide increasingly good fits to the beta decay spectrum. When an allowance for a non-zero bias  $b$  is made, all the four alpha spectra provide equally good fits ( $\chi^2_N \approx 1$ ), modulo the shift  $E_\alpha \rightarrow E_\alpha + b$ . The dotted curve, which also provides a good fit for zero bias, corresponds to the spectrum WA2 using the second Barker's calibration [19]. The main difference among the four  $\alpha$  particle data sets can thus be ascribed to small biases in the measured  $\alpha$  energies.

The natural choice for the optimal  $\alpha$  particle energy spectrum is seen to be, in Fig. 3, WA1 with  $b = +0.025$  MeV. This is our choice for the experimental input data in the calculation of the “best” neutrino spectrum. An additional variation of  $b$  equal to  $\pm 0.035$  MeV produces a  $\Delta\chi^2 = 9$  increase in the fit to the  $\beta^+$  spectrum, defining a  $\pm 3\sigma$  range for  $b$ .

We have studied the sensitivity of the  $\chi^2$  fit to the low-statistics bins by excluding up to ten bins in the high-energy part of the positron spectrum; the highest-energy bins represent 4.5% of the experimental counts. The central values of the bias  $b$  in these fits (excluding some or all of the ten highest-energy bins) are spread by  $\pm 0.005$  MeV around  $b = 0.025$  MeV, with a  $3\sigma$  error that can be as large as 0.047 MeV when all ten bins are excluded.

TABLE I. The spectrum  $\lambda$  of solar neutrinos from the decay of  $^8\text{B}$ , together with the spectra  $\lambda^\pm$  associated with the total  $\pm 3\sigma$  uncertainties. The neutrino energy  $E_\nu$  is MeV and  $\lambda^{(\pm)}(E_\nu)$  is the probability that a neutrino with energy  $E_\nu$  is emitted between  $E_\nu \pm 0.05$  MeV. A computer-readable version of this table is available at the WWW site <http://www.sns.ias.edu/~jnb/neutrino.html>.

$E_\nu$	$\lambda(E_\nu)$	$\lambda^+(E_\nu)$	$\lambda^-(E_\nu)$	$E_\nu$	$\lambda(E_\nu)$	$\lambda^+(E_\nu)$	$\lambda^-(E_\nu)$
0.1	0.000202	0.000228	0.000168	5.3	0.125007	0.127846	0.122182
0.2	0.000742	0.000800	0.000636	5.4	0.126201	0.128969	0.123438
0.3	0.001522	0.001619	0.001376	5.5	0.127287	0.129980	0.124592
0.4	0.002516	0.002708	0.002356	5.6	0.128265	0.130876	0.125643
0.5	0.003775	0.004058	0.003543	5.7	0.129134	0.131659	0.126590
0.6	0.005254	0.005628	0.004924	5.8	0.129893	0.132329	0.127432
0.7	0.006938	0.007398	0.006514	5.9	0.130544	0.132885	0.128170
0.8	0.008804	0.009357	0.008282	6.0	0.131085	0.133327	0.128802
0.9	0.010835	0.011494	0.010219	6.1	0.131517	0.133656	0.129329
1.0	0.013020	0.013795	0.012304	6.2	0.131839	0.133870	0.129751
1.1	0.015348	0.016242	0.014525	6.3	0.132052	0.133972	0.130069
1.2	0.017809	0.018816	0.016871	6.4	0.132158	0.133961	0.130282
1.3	0.020386	0.021508	0.019334	6.5	0.132155	0.133839	0.130391
1.4	0.023066	0.024308	0.021902	6.6	0.132045	0.133607	0.130395
1.5	0.025840	0.027201	0.024564	6.7	0.131830	0.133265	0.130297
1.6	0.028696	0.030170	0.027306	6.8	0.131508	0.132815	0.130096
1.7	0.031624	0.033211	0.030121	6.9	0.131083	0.132258	0.129795
1.8	0.034611	0.036312	0.033001	7.0	0.130555	0.131596	0.129393
1.9	0.037650	0.039465	0.035934	7.1	0.129925	0.130829	0.128892
2.0	0.040733	0.042659	0.038910	7.2	0.129196	0.129961	0.128294
2.1	0.043851	0.045885	0.041923	7.3	0.128368	0.128992	0.127599
2.2	0.046996	0.049133	0.044965	7.4	0.127443	0.127925	0.126809
2.3	0.050159	0.052398	0.048028	7.5	0.126423	0.126761	0.125927
2.4	0.053332	0.055669	0.051106	7.6	0.125310	0.125502	0.124952
2.5	0.056509	0.058939	0.054190	7.7	0.124106	0.124152	0.123887
2.6	0.059681	0.062202	0.057274	7.8	0.122813	0.122712	0.122734
2.7	0.062844	0.065450	0.060352	7.9	0.121433	0.121186	0.121496
2.8	0.065989	0.068678	0.063418	8.0	0.119968	0.119574	0.120172
2.9	0.069112	0.071877	0.066464	8.1	0.118422	0.117881	0.118768
3.0	0.072206	0.075040	0.069486	8.2	0.116796	0.116108	0.117284
3.1	0.075265	0.078163	0.072479	8.3	0.115094	0.114259	0.115722
3.2	0.078282	0.081238	0.075436	8.4	0.113317	0.112337	0.114086
3.3	0.081253	0.084263	0.078353	8.5	0.111468	0.110345	0.112378
3.4	0.084173	0.087230	0.081224	8.6	0.109552	0.108286	0.110600
3.5	0.087038	0.090136	0.084044	8.7	0.107570	0.106164	0.108755
3.6	0.089841	0.092976	0.086809	8.8	0.105525	0.103980	0.106847
3.7	0.092580	0.095746	0.089516	8.9	0.103421	0.101740	0.104877
3.8	0.095251	0.098441	0.092159	9.0	0.101261	0.099446	0.102849
3.9	0.097851	0.101059	0.094736	9.1	0.099047	0.097101	0.100765
4.0	0.100374	0.103595	0.097243	9.2	0.096784	0.094710	0.098629
4.1	0.102818	0.106045	0.099677	9.3	0.094475	0.092276	0.096444
4.2	0.105180	0.108408	0.102034	9.4	0.092122	0.089802	0.094213
4.3	0.107457	0.110678	0.104311	9.5	0.089731	0.087295	0.091940
4.4	0.109645	0.112855	0.106506	9.6	0.087303	0.084756	0.089626
4.5	0.111742	0.114935	0.108617	9.7	0.084844	0.082189	0.087277
4.6	0.113747	0.116916	0.110640	9.8	0.082355	0.079598	0.084895
4.7	0.115657	0.118796	0.112572	9.9	0.079842	0.076987	0.082484
4.8	0.117469	0.120572	0.114414	10.0	0.077308	0.074361	0.080047
4.9	0.119181	0.122243	0.116162	10.1	0.074758	0.071723	0.077588
5.0	0.120793	0.123808	0.117814	10.2	0.072194	0.069078	0.075110
5.1	0.122302	0.125264	0.119369	10.3	0.069620	0.066429	0.072617
5.2	0.123707	0.126611	0.120825	10.4	0.067041	0.063780	0.070113

TABLE I. (*Continued.*)

$E_\nu$	$\lambda(E_\nu)$	$\lambda^+(E_\nu)$	$\lambda^-(E_\nu)$	$E_\nu$	$\lambda(E_\nu)$	$\lambda^+(E_\nu)$	$\lambda^-(E_\nu)$
10.5	0.064460	0.061137	0.067602	13.3	0.007102	0.005267	0.009190
10.6	0.061881	0.058503	0.065087	13.4	0.006073	0.004400	0.008011
10.7	0.059309	0.055882	0.062572	13.5	0.005138	0.003630	0.006920
10.8	0.056747	0.053279	0.060061	13.6	0.004296	0.002956	0.005922
10.9	0.054199	0.050698	0.057557	13.7	0.003548	0.002374	0.005014
11.0	0.051670	0.048142	0.055065	13.8	0.002892	0.001880	0.004196
11.1	0.049162	0.045617	0.052587	13.9	0.002325	0.001469	0.003468
11.2	0.046681	0.043126	0.050129	14.0	0.001843	0.001133	0.002830
11.3	0.044231	0.040672	0.047693	14.1	0.001442	0.000863	0.002277
11.4	0.041814	0.038262	0.045283	14.2	0.001113	0.000650	0.001807
11.5	0.039435	0.035897	0.042904	14.3	0.000849	0.000485	0.001415
11.6	0.037097	0.033583	0.040559	14.4	0.000640	0.000358	0.001094
11.7	0.034805	0.031322	0.038251	14.5	0.000478	0.000263	0.000835
11.8	0.032563	0.029120	0.035984	14.6	0.000354	0.000190	0.000630
11.9	0.030373	0.026979	0.033762	14.7	0.000259	0.000137	0.000471
12.0	0.028240	0.024904	0.031588	14.8	0.000188	0.000097	0.000349
12.1	0.026167	0.022897	0.029466	14.9	0.000135	0.000068	0.000256
12.2	0.024158	0.020962	0.027399	15.0	0.000096	0.000047	0.000186
12.3	0.022216	0.019103	0.025391	15.1	0.000067	0.000031	0.000134
12.4	0.020343	0.017322	0.023445	15.2	0.000047	0.000021	0.000095
12.5	0.018544	0.015623	0.021564	15.3	0.000031	0.000013	0.000067
12.6	0.016821	0.014007	0.019751	15.4	0.000021	0.000008	0.000046
12.7	0.015177	0.012481	0.018009	15.5	0.000014	0.000005	0.000031
12.8	0.013614	0.011045	0.016340	15.6	0.000009	0.000003	0.000021
12.9	0.012134	0.009700	0.014748	15.7	0.000005	0.000002	0.000014
13.0	0.010741	0.008448	0.013235	15.8	0.000003	0.000001	0.000009
13.1	0.009435	0.007291	0.011803	15.9	0.000002	0.000000	0.000005
13.2	0.008223	0.006231	0.010454	16.0	0.000001	0.000000	0.000003

The Kolmogorov-Smirnov (KS) test provides a non-parametric (bin-free) way of determining the goodness of fit of two distributions. We have therefore applied a KS test to the best-fit (unbinned) normalized spectrum. We obtain a  $3\sigma$  error of  $\pm 0.056$  MeV for the bias  $b$ . We adopt this error  $\pm 0.056$  MeV as a conservative but relevant  $3\sigma$  estimate.

Figure 4 shows the experimental beta decay spectrum [12] (dots with  $1\sigma$  statistical error bars), the best-fit theoretical spectrum (solid curve, obtained by using WA1 data with  $b=0.025$  MeV), and the “ $\pm 3\sigma$ ” theoretical spectra (dotted curves, WA1 data with  $b=0.025\pm 0.056$  MeV).

As discussed in Sec. II A, the  $\beta$ -decay reference spectrum is affected by a maximum energy calibration uncertainty  $\delta E_\beta = \pm 0.090$  MeV ( $3\sigma$ ). An error  $\pm \delta E_\beta$  corresponds to an error  $\mp 2\delta E_\alpha$  in the  ${}^8\text{B}(\beta^+){}^8\text{Be}(2\alpha)$ -decay chain. As a consequence, the total range of the  $\alpha$  energy bias  $b$  gets slightly enlarged:  $b=0.025\pm 0.056\pm 0.045=0.025\pm 0.072$  MeV, where the two (independent) errors have been added in quadrature.

The estimated  $\pm 3\sigma$  range for  $b$  ( $\pm 0.072$  MeV) is approximately equal to the spread in the peaks of the experimental alpha decay spectra ( $\pm 0.08$  MeV) discussed at the beginning of this section.

### III. ${}^8\text{B}$ STANDARD NEUTRINO SPECTRUM AND ITS UNCERTAINTIES

In this section, the main results of the present paper are presented: a best (standard)  ${}^8\text{B}$  neutrino spectrum  $\lambda(E_\nu)$ ,

together with two supplementary spectra  $\lambda^+(E_\nu)$  and  $\lambda^-(E_\nu)$  obtained by stretching the total uncertainties to their  $\pm 3\sigma$  limits. These spectra are given both in the figures and tables. The effects of the individual experimental and theoretical uncertainties are also discussed and illustrated graphically.

#### A. Optimal neutrino spectrum and its $3\sigma$ deviations

The successive calculations of the  ${}^8\text{B}$  normalized neutrino spectrum  $\lambda(E_\nu)$  included—besides the phase space factor [11]—the intermediate state smearing [11], the proper Fermi function [11,13], and the forbidden corrections to the allowed transition [14].

Napolitano *et al.* [12] pointed out the potential relevance of radiative corrections, although only those corresponding to the  ${}^8\text{B}$  positron spectrum [28] were known at the time. Here we include the appropriate radiative corrections to the  ${}^8\text{B}$  neutrino spectrum that have been recently calculated in [29]. These corrections are smaller (due to a cancellation between real and virtual photon contributions [29]), and with a milder energy dependence, than the corrections that apply when the charged lepton is detected in  $\beta$ -decay [28]. As we shall see below, their inclusion makes no significant difference in the calculation.

The optimal-input alpha decay data, as discussed in the previous section, are taken as WA1 with an energy bias  $b$  having a central value of 0.025 MeV and a  $\pm 3\sigma$  experimen-

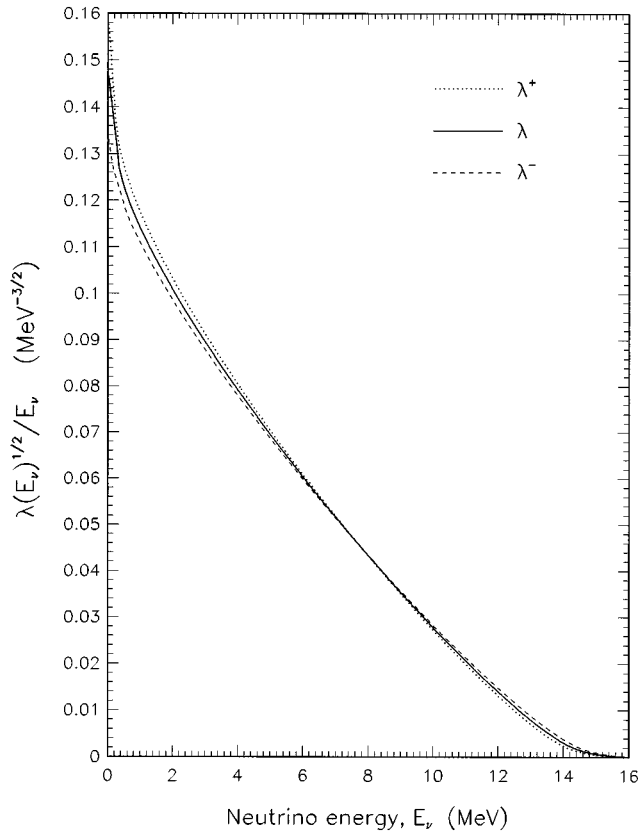


FIG. 6. The spectra  $\lambda$ ,  $\lambda^+$ , and  $\lambda^-$ , shown as a Kurie plot.

tal uncertainty  $\Delta b = \pm 0.072$  MeV (determined by the fit to the  $\beta$ -decay data). We anticipate (see below) that the inclusion of the maximal theoretical uncertainties can be mimicked by enlarging the above range to  $\Delta b = \pm 0.104$  MeV. The ‘‘ $3\sigma$  different’’ neutrino spectra  $\lambda^+$  and  $\lambda^-$  are calculated for the extreme values of  $\Delta b$  ( $+0.104$ , and  $-0.104$  MeV, respectively).

The results for the normalized neutrino spectra are shown in Fig. 5. (The spectra all happen to be almost coincident at about half of the maximum energy.) Numerical values of  $\lambda$ ,  $\lambda^+$  and  $\lambda^-$  are reported in Table I. A computer-readable version of Table I is available at the WWW site <http://www.sns.ias.edu/~jnb/neutrino.html>.

An alternative representation of the above neutrino spectra, in which the trivial part of the energy dependence is factorized out, is shown in Fig. 6 (a Kurie plot<sup>1</sup>), where the ordinate is  $\sqrt{\lambda}/E_\nu$ . Notice the deviation from a straight line; the deviation is primarily due to the smearing over the intermediate broad state of  $^8\text{Be}$ .

A representation of the integral spectrum is shown in Fig. 7, where the fraction  $f$  of  $^8\text{B}$  neutrinos produced above a given neutrino energy threshold  $E_{\text{th}}$  [ $f = \int_{E_{\text{th}}}^{\infty} dE_\nu \lambda(E_\nu)$ ] is plotted as function of  $E_{\text{th}}$ .

<sup>1</sup>We have not divided the spectrum by the Fermi function as is usual in plotting beta decay spectra. In the present case, the Fermi function would have to be averaged over a range of positron energies because of the width of the final ( $2^+$ ) state in  $^8\text{Be}$ .

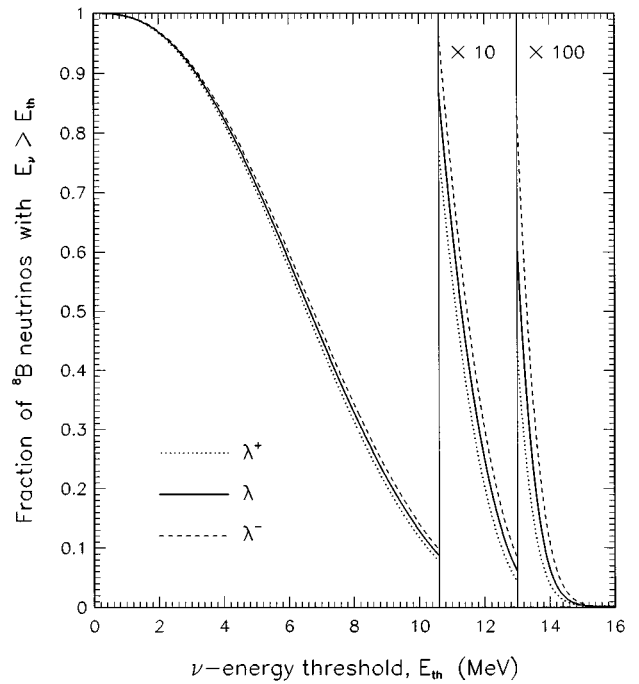


FIG. 7. Fraction of  $^8\text{B}$  neutrinos produced with energy  $E_\nu$  above a given threshold  $E_{\text{th}}$ .

### B. Spectrum uncertainties: Experimental and theoretical components

The effect of varying the input alpha decay data with respect to the optimal choice (WA1 with bias  $b=0.025$ ) is shown in Fig. 8, where the solid line represents the standard spectrum  $\lambda$ , and crosses are placed at representative points

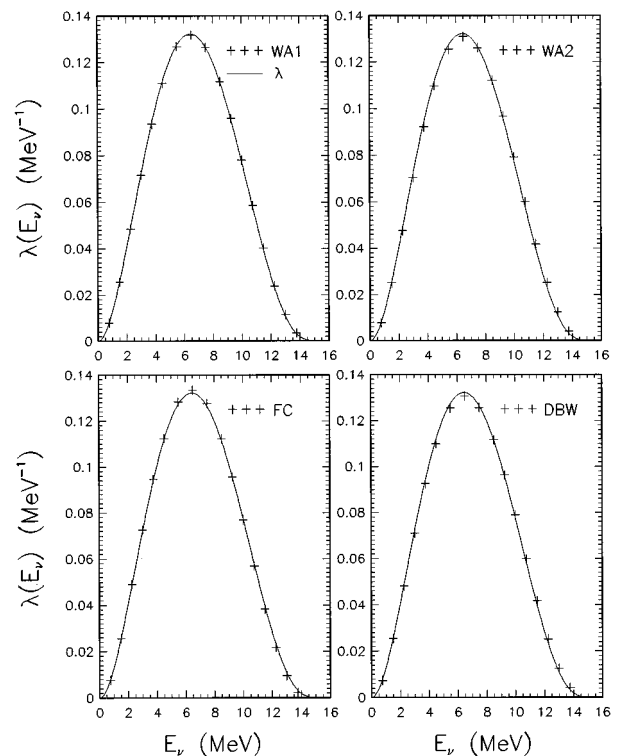


FIG. 8. Variations in the standard neutrino spectrum  $\lambda$  (solid line) induced by different input data sets (crosses).

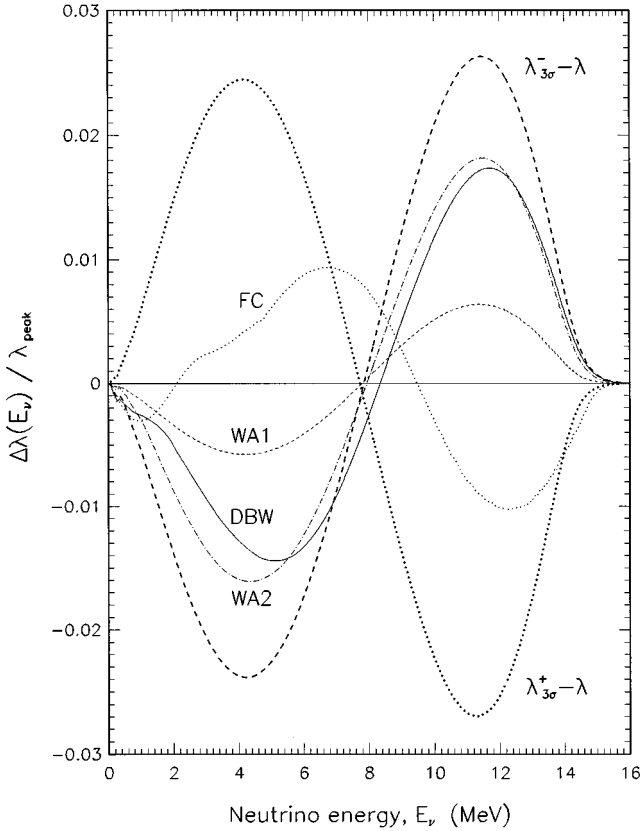


FIG. 9. Variations  $\Delta\lambda$  in the standard neutrino spectrum  $\lambda$  induced by different input data sets, divided by the peak value of  $\lambda$  ( $\lambda_{\text{peak}}$ ). The maximum ( $\pm 3\sigma$ ) differences  $\lambda^{\pm} - \lambda$  are also shown.

along the spectra  $\lambda'$  obtained with WA1, WA2, FC, and DBW input data (with no bias). The differences  $\Delta\lambda = \lambda' - \lambda$  are very small, and can be best appreciated in an expanded scale in Fig. 9, where the dimensionless quantity  $\Delta\lambda/\lambda_{\text{peak}}$  is plotted [ $\lambda_{\text{peak}} = \max\lambda(E_\nu)$ ].

Figure 9 also shows the  $\pm 3\sigma$  deviations  $(\lambda^{\pm} - \lambda)/\lambda_{\text{peak}}$ . These deviations are similar to sinusoidal curves, with a maximum amplitude of  $\sim 2.5\%$ . The average value of the absolute deviation is thus  $\langle |\Delta\lambda/\lambda_{\text{peak}}| \rangle \approx (2/\pi) |\Delta\lambda|_{\text{max}}/\lambda_{\text{peak}} \approx 1.6\%$  at  $3\sigma$ . The difference between the Bahcall-Holstein [14] spectrum  $\lambda_{\text{BH}}$  and the best-fit spectrum  $\lambda$  can also be represented well by a sinusoidal curve (like those shown in Fig. 9). The amplitude of the difference  $\lambda_{\text{BH}} - \lambda$  is  $\sim 0.7\sigma$ , to be compared with the effective  $3\sigma$  differences  $\lambda^{\pm} - \lambda$  shown in Fig. 9. Similarly, the difference between the spectrum  $\lambda_{\text{N}}$  calculated by Napolitano *et al.* in [12] and the standard spectrum  $\lambda$  is about  $1.4\sigma$ .

Notice that the curve FC in Fig. 9 is somewhat irregular and “out of phase” (about  $\frac{1}{4}$  of a semiperiod) with respect to the  $\pm 3\sigma$  sinusoids. The irregularity is due to the scatter of the FC data points. The dephasing can be traced back to the fact that the FC data set has very few low-energy counts, being limited to  $E_\alpha \gtrsim 1.2$  MeV. We have verified that the curve FC in Fig. 9 is “rephased” if the FC alpha spectrum of Fig. 2 is artificially prolonged to lower energies. We have also computed neutrino spectra with “mixed alpha data,” namely, with WA1 data for  $E_\alpha > E_{\text{peak}}$  matched to DBW data for  $E_\alpha < E_{\text{peak}}$  (and vice versa). We found that the spectral

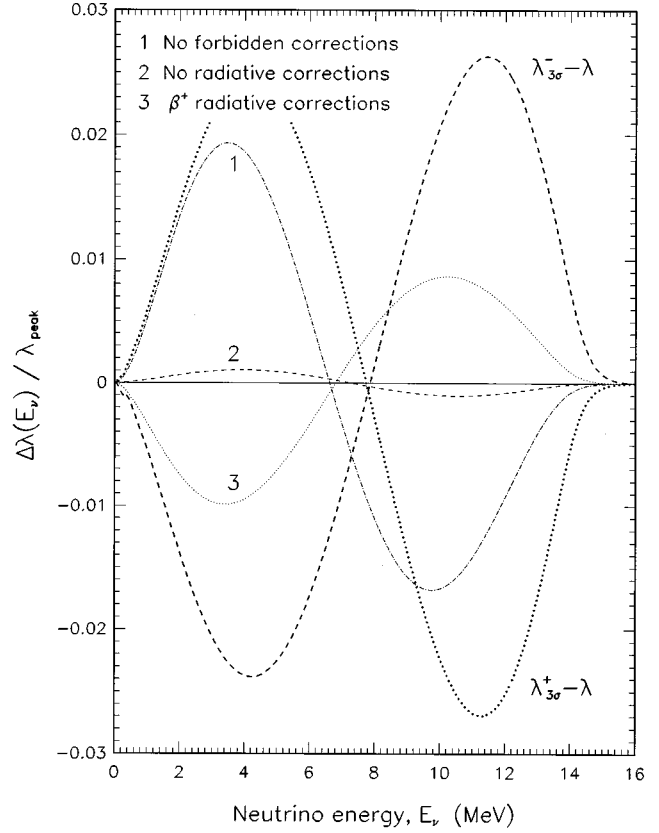


FIG. 10. Variations  $\Delta\lambda$  in the neutrino spectrum induced by drastic changes in the theoretical computation, shown in the same scale as Fig. 9. See the text for details.

differences can always be reabsorbed in a uniform bias  $b$  to a very good approximation, with residual differences of  $\lesssim 0.015$  MeV with respect to the “unmixed” original data. We conclude that the low-energy part of the experimental alpha decay spectrum (that affects particularly the high-energy tail of the neutrino spectrum) is sufficiently well known for our purposes, and that the alpha spectra uncertainties can be effectively parametrized as a uniform energy offset  $b$ .

The effects of radical assumptions about the correctness of the theoretical calculations beyond the (phase space)  $\times$  (Fermi function) approximation are shown in Fig. 10, on the same scale as Fig. 9. The curves labeled 1 and 2 represent the shifts  $\Delta\lambda/\lambda_{\text{peak}}$  obtained by setting to zero the forbidden or the radiative corrections, respectively. For curve 3, the radiative corrections were (inappropriately) assumed to be the same as for the positron detection case [28] (as was also done in [12]); the present exercise is intended to account roughly for a hypothetical situation in which the cancellation between real and virtual photon contributions might not be as effective as computed in [29].

The maximum theoretical deviation (curve 1 in Fig. 10) is obtained by excluding the forbidden corrections altogether. We have verified that this deviation can be mimicked by recalculating the neutrino energy spectrum with an additional energy bias  $\Delta b_{\text{theor}} \approx 0.075$  MeV. This value is comparable to the estimated  $3\sigma$  experimental uncertainty evaluated in Sec. II C,  $\Delta b_{\text{expt}} \approx 0.072$ . We assume that the maximum theoretical offset,  $\Delta b_{\text{theor}}$ , corresponds to an “effective”

$3\sigma$  statistical significance. Our final best-estimate for the bias  $b$  to be applied to the reference WA1  $\alpha$ -decay spectrum is therefore:  $b = 0.025 \text{ MeV} \pm (\Delta b_{\text{expt}}^2 + \Delta b_{\text{theor}}^2)^{1/2} = 0.025 \pm 0.104 \text{ MeV}$ , as anticipated in Sec. III A.

The assignment of a ‘‘ $3\sigma$  level of significance’’ to the offset that parametrizes the total effect of the forbidden corrections is a plausible estimate. However, there is no rigorous way to estimate a  $3\sigma$  theoretical uncertainty. Our estimate is motivated by the fact that the calculation of forbidden corrections in beta decay is not made purely from first principles (strong and electroweak Lagrangian), unlike the QED radiative corrections. The evaluation of the forbidden terms makes use of approximate symmetries to expand the weak nuclear current in terms of a few nuclear form factors, which are evaluated using nuclear models and difficult  $\beta$ - $\alpha$  correlation experiments (see [14] and references therein).

If the reader prefers to adopt a smaller or larger estimate for the theoretical uncertainty, a simple prescription for estimating the changes in the inferred uncertainties is given below. The prescription is based upon linear error propagation and generally gives agreement with an exact numerical calculation to a fractional accuracy of about 5% or better in the change induced by the rescaling of the error. Recalculate the total  $3\sigma$  range for the bias  $\Delta b = (\Delta b_{\text{expt}}^2 + \Delta b_{\text{theor}}^2)^{1/2}$ , with  $\Delta b_{\text{expt}} = 0.072 \text{ MeV}$  and the reader’s preferred estimate for  $\Delta b_{\text{theor}}$ . Then rescale by a factor  $f = \Delta b / (0.104 \text{ MeV})$  all the  $^8\text{B}$ -related  $3\sigma$  total uncertainties quoted in this paper. For example, the  $3\sigma$  spectral deviations from the best-estimated neutrino spectrum shape,  $\lambda^\pm(E_\nu) - \lambda(E_\nu)$ , become  $f[\lambda^\pm(E_\nu) - \lambda(E_\nu)]$ . Notice that the rescaling factor is at least  $f = 0.69$ , which is obtained by setting  $\Delta b_{\text{theor}} = 0$ .

A final remark is in order. The relative contribution of the different  $2^+$  states of  $^8\text{Be}$  in the  $\alpha$ -decay spectrum (see Fig. 1) has been analyzed by Barker [17,19] and Warburton [18] within the  $R$ -matrix formalism. Their results are not in complete agreement, the fitted amplitude of the intermediate states being sensitive to the input data (see, e.g., the discussion in [19]). In particular,  $R$ -matrix fits are very sensitive to the absolute energy calibration, as well as to the tails of the alpha decay spectrum. In our calculation of the neutrino spectrum, the absolute  $\alpha$  energy is allowed to vary within the quoted uncertainties ( $\pm 0.104 \text{ MeV}$ ). The tails of the alpha decay spectrum are not decisive for our purposes. We are not really interested in separating the relative contributions of the  $2^+$  states; we just rely upon the global population of the  $2^+$  states as derived from the *experimental*  $\alpha$ -decay data. We conclude that the disagreement between the theoretical  $R$ -matrix fits [17–19] is not an issue in our calculation of the  $^8\text{B}$  neutrino spectrum.

#### IV. ABSORPTION CROSS SECTION OF $^8\text{B}$ NEUTRINOS IN $^{37}\text{Cl}$ AND $^{71}\text{Ga}$

In this section, we present improved calculations of the  $^8\text{B}$  neutrino absorption cross section for chlorine and for gallium. Recent calculations of the chlorine absorption cross section were made by Bahcall and Holstein [14], García *et al.* [30], and Aufderheide *et al.* [31]; the results of earlier calculations can be found in [11,13,32–36]. The most recent

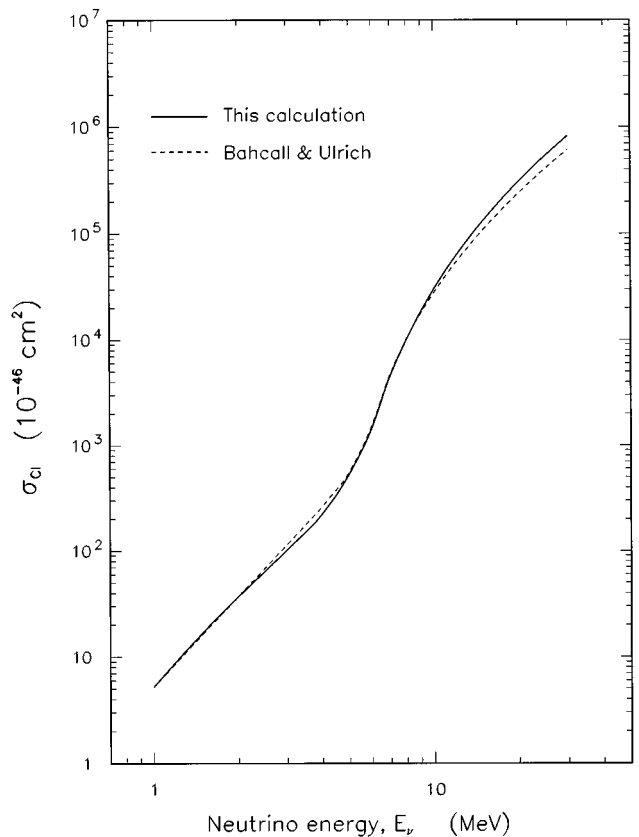


FIG. 11. Absorption cross section in chlorine (solid line) as a function of the neutrino energy. The dashed line refers to the Bahcall-Ulrich [37] calculation.

previous calculation of the gallium cross section  $\sigma_{\text{Ga}}$  was by Bahcall and Ulrich [37].

Transitions to excited states dominate the total cross section in either of the absorption processes  $^{37}\text{Cl}(\nu, e)^{37}\text{Ar}$  and  $^{71}\text{Ga}(\nu, e)^{71}\text{Ge}$ . The Gamow-Teller transition strengths,  $B(\text{GT})$  can be estimated from the rates of the analogous charge-exchange ( $p, n$ ) reactions. For the  $A=37$  system, these transition matrix elements can be determined experimentally by studying the  $^{37}\text{Ca}(\beta^+)^{37}\text{K}$  transition [32,11], which is the isospin mirror process of  $^{37}\text{Cl}(\nu, e)^{37}\text{Ar}$ . The interested reader is referred to the recent review in [38] for a more extensive discussion of these processes.

##### A. Absorption cross section for chlorine

Including for the first time-forbidden corrections, Bahcall and Holstein [14] calculated the  $^8\text{B}$  neutrino cross section on chlorine and obtained

$$\sigma_{\text{Cl}} = (1.06 \pm 0.10) \times 10^{-42} \text{ cm}^2. \quad (1)$$

The quoted uncertainties represented the maximum estimated error ( $3\sigma$ ). The calculation made use of the  $B(\text{GT})$  value derived from the  $^{37}\text{Ca}$   $\beta$ -decay, as reported by Sextro *et al.* in [34]. The estimated  $3\sigma$  error ( $\pm 0.10$ ) had two components,  $\pm 0.08$  from  $^8\text{Be}$   $\alpha$ -decay data and  $\pm 0.06$  from  $^{37}\text{Ca}$   $\beta$ -decay data uncertainties, to be added in quadrature.

Using the same low-energy data [34] as in [14], and the spectra  $\lambda$ ,  $\lambda^+$ , and  $\lambda^-$  reported in Table I, we find

TABLE II. Values of the absorption cross section in chlorine, in units of  $10^{-42}$  cm<sup>2</sup>, for representative values of the neutrino energy. The second column refers to the calculation in the present paper. The third column refers to the Bahcall-Ulrich (BU) [37] calculation.

$E_\nu$ (MeV)	$\sigma_{\text{Cl}}$	$\sigma_{\text{Cl}}(\text{BU})$
1	$5.21 \times 10^0$	$5.21 \times 10^0$
2	$3.70 \times 10^1$	$3.70 \times 10^1$
3	$1.02 \times 10^2$	$1.15 \times 10^2$
4	$2.23 \times 10^2$	$2.63 \times 10^2$
5	$5.38 \times 10^2$	$5.63 \times 10^2$
6	$1.44 \times 10^3$	$1.52 \times 10^3$
7	$4.62 \times 10^3$	$4.76 \times 10^3$
8	$1.01 \times 10^4$	$1.02 \times 10^4$
9	$1.85 \times 10^4$	$1.79 \times 10^4$
10	$3.00 \times 10^4$	$2.77 \times 10^4$
11	$4.45 \times 10^4$	$3.97 \times 10^4$
12	$6.21 \times 10^4$	$5.38 \times 10^4$
13	$8.27 \times 10^4$	$7.00 \times 10^4$
14	$1.06 \times 10^5$	$8.83 \times 10^4$
15	$1.33 \times 10^5$	$1.09 \times 10^5$
16	$1.62 \times 10^5$	$1.31 \times 10^5$
18	$2.28 \times 10^5$	$1.81 \times 10^5$
20	$3.05 \times 10^5$	$2.38 \times 10^5$
30	$8.20 \times 10^5$	$6.11 \times 10^5$

$\sigma_{\text{Cl}} = (1.08 \pm 0.15) \times 10^{-42}$  cm<sup>2</sup>. The best-estimate calculated cross sections differ by 2%. The  $3\sigma$  error component from <sup>8</sup>Be( $2\alpha$ )-decay data is  $\pm 0.07$ .

Recently, new experiments have been carried out to determine more precisely the  $B(\text{GT})$  strengths in <sup>37</sup>Cl( $p, n$ ), <sup>37</sup>Ar [36] and <sup>37</sup>Ca( $\beta^+$ ), <sup>37</sup>K [30] processes. Taken at face values, the  $B(\text{GT})$  strengths derived by the different experiments [30,34,36] were not in good agreement. Critical examinations [39] of the data analyses, as well as supplementary data [40], may have led to a satisfactory understanding [31] of the low-energy levels and their  $B(\text{GT})$  strengths in the  $A=37$  system.

Using the latest available data [31] and the neutrino spectra  $\lambda^{(\pm)}$  calculated here, we find

$$\sigma_{\text{Cl}} = (1.14 \pm 0.11) \times 10^{-42} \text{ cm}^2. \quad (2)$$

Equation (2) represents our best estimate, and the associated  $3\sigma$  uncertainties, for the <sup>8</sup>B neutrino absorption cross section on chlorine. The contribution to the total error from the measured  $B(\text{GT})$  values is assumed to be  $\pm 0.08$ , as in the analysis [31]. The difference between the values of the chlorine absorption cross section in Eq. (1) and Eq. (2) is 7%, well within the quoted errors.

Figure 11 shows the energy dependence of our best-estimate chlorine cross section (solid line). Values of  $\sigma_{\text{Cl}}$  for representative neutrino energies are also given in Table II. The difference between the present and the previous calculation of the *energy-dependent* cross section by Bahcall and Ulrich [37] (dashed line in Fig. 11) is less than 20% for  $E_\nu < 16$  MeV. The differences are largest at the highest energies since the newer data include transitions to higher ex-

TABLE III. Values of the <sup>8</sup>B neutrino absorption cross section for chlorine ( $\sigma_{\text{Cl}}$ ), as calculated by various authors. The first and second (when given) error components  $\epsilon_{\text{GT}}$  and  $\epsilon_{\text{B}}$  are to be added in quadrature; they refer to the estimated uncertainties from the Gamow-Teller (GT) strengths and from the <sup>8</sup>B neutrino spectrum, respectively. When the definitions of the errors given in the original papers were sufficiently precise, we have indicated (in parentheses) that we are quoting  $3\sigma$  errors.

Year	Author(s)	Ref.	$\sigma_{\text{Cl}} \pm \epsilon_{\text{GT}} \pm \epsilon_{\text{B}}$ ( $10^{-42}$ cm <sup>2</sup> )
1964	Bahcall	[32]	$1.27 \pm 0.31$
1964	Bahcall	[11]	$1.30 \pm 0.29$
1966	Bahcall	[33]	$1.35 \pm 0.10$
1974	Sextro <i>et al.</i>	[34]	1.31
1977	Haxton and Donnelly	[35]	$1.27 \pm 0.22 \pm 0.06$
1978	Bahcall	[13]	$1.08 \pm 0.10$
1981	Rapaport <i>et al.</i>	[36]	$0.98 \pm 0.07$
1986	Bahcall and Holstein	[14]	$1.06 \pm 0.06 \pm 0.08$ [ $3\sigma$ ]
1991	García <i>et al.</i>	[30]	$1.09 \pm 0.03$
1994	Aufderheide <i>et al.</i>	[31]	$1.11 \pm 0.08$ [ $3\sigma$ ]
1996	Bahcall <i>et al.</i>	This work	$1.14 \pm 0.08 \pm 0.08$ [ $3\sigma$ ]

citation states in <sup>37</sup>Ar that were not determined in the previous experiments (see [30,39,31]).

To give the reader some perspective on how the <sup>8</sup>B neutrino spectrum and the chlorine absorption cross section have changed with time, we give in Table III all the published values of  $\sigma_{\text{Cl}}$  with which we are familiar. The calculated cross sections have been approximately constant, within the estimated errors, since 1978, although there have been numerous refinements (which are described in [13,14,36,30,31]). The reasons for the relatively significant change in the 1978 best-estimated value [13] with respect to the earlier calculations [11,33–35] are described in the last paragraph of Sec. IV B 3 in [13].

### B. Absorption cross section for gallium

The <sup>8</sup>B neutrino absorption cross section for gallium that is widely used was calculated by Bahcall and Ulrich [37] and is

$$\sigma_{\text{Ga}} = (2.43_{-1.1}^{+2.1}) \times 10^{-42} \text{ cm}^2, \quad (3)$$

where the quoted uncertainties represented the maximum estimated errors ( $3\sigma$ ). The  $B(\text{GT})$  values used in the quoted calculation were taken from a <sup>71</sup>Ga( $p, n$ ), <sup>71</sup>Ge experiment performed by Krofcheck *et al.* [41].

The only important recently published experimental development with which we are familiar is the recent <sup>51</sup>Cr source experiment for the GALLEX detector [42]. Hata and Haxton [43] have shown that the measurements with the chromium source are consistent with the  $B(\text{GT})$  values for the first two excited states that were inferred by Krofcheck *et al.* [41].

Therefore we repeat the Bahcall-Ulrich calculation [Eq. (3)] using the best <sup>8</sup>B neutrino spectrum from the present paper. We find

$$\sigma_{\text{Ga}} = (2.46_{-1.1}^{+2.1}) \times 10^{-42} \text{ cm}^2. \quad (4)$$

The change in the best-estimate cross section is only  $\sim 1\%$  [relative to Eq. (3)], which is much smaller than the guessed systematic errors, which represent uncertainties in the interpretation of the  $(p, n)$  measurements.

## V. SUMMARY

In the previous sections, the spectrum of neutrinos produced in the  ${}^8\text{B}(\beta^+){}^8\text{Be}(2\alpha)$  decay has been computed, using state-of-the-art theory of beta decay. The laboratory data on the associated positron spectrum have been used to choose an optimal data set among the different measured  ${}^8\text{Be}(2\alpha)$  decay spectra. The experimental and theoretical uncertainties can both be represented well as an energy shift ( $b$ ) in the  $\alpha$ -decay data. The total  $\pm 3\sigma$  range for this shift (bias) has been conservatively estimated to be  $\pm 0.104$  MeV. A best-fitting standard spectrum  $\lambda$  has been computed, as well as the “effective  $\pm 3\sigma$ ” neutrino spectral shapes  $\lambda^+$  and  $\lambda^-$  ( $\lambda^\pm - \lambda = 3$  standard deviations). The standard spectrum  $\lambda$  differs by about  $0.7\sigma$  from the Bahcall-Holstein neutrino spectrum [14] and by about  $1.4\sigma$  from the spectrum of Napolitano *et al.* [12].

The  ${}^8\text{B}$  neutrino absorption cross section for chlorine calculated with the best-fitting spectrum derived here and with the most recent data on the low-lying states in the  $A=37$  system is  $\sigma_{\text{Cl}} = (1.14 \pm 0.11) \times 10^{-42} \text{ cm}^2$  ( $3\sigma$ ). This result is in agreement with the estimates derived in 1964 (see Table III). The best-estimate gallium absorption cross section is  $\sigma_{\text{Ga}} = (2.46_{-1.1}^{+2.1}) \times 10^{-42} \text{ cm}^2$  ( $3\sigma$ ).

Many readers would prefer to quote  $1\sigma$  rather than  $3\sigma$  errors. To a good approximation,  $1\sigma$  errors can be obtained

from our quoted  $3\sigma$  values by dividing by 3. Moreover,  $[\lambda^\pm(E_\nu) - \lambda(E_\nu)]_{1\sigma} \approx [\lambda^\pm(E_\nu) - \lambda(E_\nu)]_{3\sigma}/3$ .

All the available experimental data on the  ${}^8\text{B}(\beta^+){}^8\text{Be}(2\alpha)$ -decay are consistent within the quoted uncertainties. Higher-order contributions in the theoretical calculation of the  ${}^8\text{B}$  neutrino spectrum should be very small. Any measured deviation of the  ${}^8\text{B}$  solar neutrino spectrum in excess of the conservative limits given in this paper could be considered as evidence for new physics beyond the standard electroweak model, at an effective significance level greater than three standard deviations.

## ACKNOWLEDGMENTS

We acknowledge useful discussion and correspondence with F. Ajzenberg-Selove, M. B. Aufderheide, I. S. Batkin, A. Hime, and M. K. Sundaresan. We are grateful to D. H. Wilkinson for permission to use the data in [24] and for valuable discussions. The work of J.N.B. was supported in part by NSF Grant No. PHY95-13835. The work of E.L. was supported in part by the Institute for Advanced Study through the NSF grant listed above and through the Monell Foundation, and in part by INFN. The research of E.L. was also performed under the auspices of the Theoretical Astroparticle Network, under Contract No. CHRX-CT93-0120 of the Direction General XII of the E.E.C. The work of D.E.A. at Brookhaven National Laboratory was performed under Contract No. DE-AC02-76CH00016 with the U.S. Department of Energy. The work of S.J.F. was performed under Contract No. DE-AC03-76SF00098 with the U.S. Department of Energy.

- 
- [1] R. Davis, *Prog. Part. Nucl. Phys.* **32**, 13 (1994); B. T. Cleveland *et al.*, in *Neutrino '94*, Proceedings of the 16th International Conference on Neutrino Physics and Astrophysics, Eilat, Israel, edited by A. Dar, G. Eilam, and M. Gronau [*Nucl. Phys. B (Proc. Suppl.)* **31**, 47 (1995)].
- [2] Kamiokande Collaboration, Y. Suzuki *et al.*, in *Neutrino '94* [1], p. 54; K. S. Hirata *et al.*, *Phys. Rev. D* **44**, 2241 (1991); **45**, 2170(E) (1992).
- [3] GALLEX Collaboration, P. Anselmann *et al.*, *Phys. Lett. B* **357**, 237 (1995).
- [4] SAGE Collaboration, J. S. Nico *et al.*, in *ICHEP '94*, Proceedings of the 27th International Conference on High Energy Physics, Glasgow, Scotland, edited by P. J. Bussey and I. Knowles (Institute of Physics Publishing, Bristol, 1995), Vol. II, p. 965; J. N. Abdurashitov *et al.*, *Phys. Lett. B* **328**, 234 (1994).
- [5] J. N. Bahcall, *Neutrino Astrophysics* (Cambridge University Press, Cambridge, England, 1989); J. N. Bahcall and M. H. Pinsonneault, *Rev. Mod. Phys.* **67**, 781 (1995).
- [6] J. N. Bahcall, *Phys. Lett. B* **338**, 276 (1994); N. Hata, S. Bludman, and P. Langacker, *Phys. Rev. D* **49**, 3622 (1994).
- [7] J. N. Bahcall, *Phys. Rev. D* **44**, 1644 (1991).
- [8] Y. Totsuka, “SuperKamiokande,” University of Tokyo (ICRR) Report No. ICRR-227-90-20, 1990 (unpublished).
- [9] SNO Collaboration, G. T. Ewan *et al.*, “Sudbury Neutrino Observatory Proposal,” Report No. SNO-87-12, 1987 (unpublished); “Scientific and Technical Description of the Mark II SNO Detector,” edited by E. W. Beier and D. Sinclair, Report No. SNO-89-15, 1989 (unpublished).
- [10] ICARUS Collaboration, “ICARUS II, a second-generation proton decay experiment and neutrino observatory at the Gran Sasso Laboratory,” Laboratori Nazionali del Gran Sasso (LNGS, Italy) Report No. 94/99, (unpublished) Vols. I and II; “addendum,” LNGS Report No. 95/10 (unpublished).
- [11] J. N. Bahcall, *Phys. Rev.* **135**, B137 (1964).
- [12] J. Napolitano, S. J. Freedman, and J. Camp, *Phys. Rev. C* **36**, 298 (1987).
- [13] J. N. Bahcall, *Rev. Mod. Phys.* **50**, 881 (1978).
- [14] J. N. Bahcall and B. R. Holstein, *Phys. Rev. C* **33**, 2121 (1986).
- [15] F. Ajzenberg-Selove, *Nucl. Phys.* **A490**, 1 (1988).
- [16] L. Grenacs, *Annu. Rev. Nucl. Part. Sci.* **35**, 455 (1985).
- [17] F. C. Barker, *Aust. J. Phys.* **22**, 293 (1969).
- [18] E. K. Warburton, *Phys. Rev. C* **33**, 303 (1986).
- [19] F. C. Barker, *Aust. J. Phys.* **42**, 25 (1989).
- [20] J. B. Camp, *Phys. Rev. C* **41**, 1719 (1990).
- [21] A. R. Heath and G. T. Garvey, *Phys. Rev. C* **31**, 2190 (1985).
- [22] R. E. Tribble and G. T. Garvey, *Phys. Rev. C* **12**, 967 (1975).
- [23] R. D. McKeown, G. T. Garvey, and C. A. Gagliardi, *Phys. Rev. C* **22**, 738 (1980); **26**, 2336(E) (1982).

- [24] D. H. Wilkinson and D. E. Alburger, *Phys. Rev. Lett.* **26**, 1127 (1971).
- [25] B. J. Farmer and C. M. Class, *Nucl. Phys.* **15**, 626 (1960).
- [26] L. De Braekeleer and D. Wright (unpublished data), as quoted in L. De Braekeleer *et al.*, *Phys. Rev. C* **51**, 2778 (1995).
- [27] G. J. Clark, P. B. Treacy, and S. N. Tucker, *Aust. J. Phys.* **22**, 663 (1969).
- [28] A. Sirlin, *Phys. Rev.* **164**, 1767 (1967).
- [29] I. S. Batkin and M. K. Sundaresan, *Phys. Rev. D* **52**, 5362 (1995).
- [30] A. García *et al.*, *Phys. Rev. Lett.* **67**, 3654 (1991).
- [31] M. B. Aufderheide, S. D. Bloom, D. A. Resler, and C. D. Goodman, *Phys. Rev. C* **49**, 678 (1994). We thank M. B. Aufderheide for providing us with the original data in a computer-readable form.
- [32] J. N. Bahcall, *Phys. Rev. Lett.* **12**, 300 (1964).
- [33] J. N. Bahcall, *Phys. Rev. Lett.* **17**, 398 (1966).
- [34] R. G. Sextro, R. A. Gough, and J. Cerny, *Nucl. Phys.* **A234**, 130 (1974).
- [35] W. C. Haxton and W. T. Donnelly, *Phys. Lett. B* **66**, 123 (1977).
- [36] J. Rapaport *et al.*, *Phys. Rev. Lett.* **47**, 1518 (1981).
- [37] J. N. Bahcall and R. K. Ulrich, *Rev. Mod. Phys.* **60**, 297 (1988).
- [38] K. Kubodera and S. Nozawa, *Int. J. Mod. Phys. E* **3**, 101 (1994).
- [39] E. G. Adelberger and W. C. Haxton, *Phys. Rev. C* **36**, 879 (1987); E. G. Adelberger, A. García, P. V. Magnus, and D. P. Wells, *Phys. Rev. Lett.* **67**, 3658 (1991); M. B. Aufderheide, S. D. Bloom, D. A. Resler, and C. D. Goodman, *Phys. Rev. C* **46**, 2251 (1992); J. Rapaport and E. R. Sugarbaker, *Phys. Rev. Lett.* **69**, 2444 (1992); C. D. Goodman, M. B. Aufderheide, S. D. Bloom, and D. A. Resler, *ibid.* **69**, 2445 (1992); D. P. Wells, E. G. Adelberger, P. V. Magnus, and A. García, *ibid.* **69**, 2446 (1992); S. M. Austin, N. Anantaraman, and W. G. Love, *ibid.* **73**, 30 (1994).
- [40] C. Iliadis *et al.*, *Phys. Rev. C* **48**, R1479 (1993). But, see also W. Trinder *et al.*, *Phys. Lett. B* **349**, 267 (1995); A. García *et al.*, *Phys. Rev. C* **51**, R439 (1995).
- [41] D. Krofcheck *et al.*, *Phys. Rev. Lett.* **55**, 1051 (1985); D. Krofcheck, Ph.D. thesis, 1986.
- [42] GALLEX Collaboration, P. Anselmann *et al.*, *Phys. Lett. B* **342**, 440 (1995).
- [43] N. Hata and W. Haxton, *Phys. Lett. B* **353**, 422 (1995).